Thermodynamic Analysis of the Binding of Aromatic Hydroxamic Acid Analogues to Ferric Horseradish Peroxidase†

Susan M. Aitken,‡,§ Joanne L. Turnbull,‡ M. David Percival,‡,§ and Ann M. English*,‡

Department of Chemistry and Biochemistry, Concordia University, 1455 de Maisonneuve Boulevard West, Montreal, Quebec, Canada H3G 1M8, and Department of Biochemistry and Molecular Biology, Merck Frosst Centre for Therapeutic Research, P.O. Box 1005, Pointe-Claire-Dorval, Quebec, Canada H9R-4P8

Received March 5, 2001; Revised Manuscript Received July 2, 2001

ABSTRACT: Peroxidases typically bind their reducing substrates weakly, with K_d values in the millimolar range. The binding of benzhydroxamic acid (BHA) to ferric horseradish peroxidase isoenzyme C (HRPC) [$K_d = 2.4\ \mu$M; Schonbaum, G. R. (1973) *J. Biol. Chem. 248,* 502−511] is a notable exception and has provided a useful tool for probing the environment of the peroxidase aromatic-donor-binding site and the distal heme cavity. Knowledge of the underlying thermodynamic driving forces is key to understanding the roles of the various H-bonding and hydrophobic interactions in substrate binding. The isothermal titration calorimetry results of this study on the binding of aromatic hydroxamic acid analogues to ferric HRPC under nonturnover conditions (no H_2O_2 present) confirm the significance of H-bonding interactions in the distal heme cavity in complex stabilization. For example, the binding of BHA to HRPC is enthalpically driven at pH 7.0, with the H-bond to the distal Arg38 providing the largest contribution (6.74 kcal/mol) to the binding energy. The overall relatively weak binding of the hydroxamic acid analogues to HRPC is due to large entropic barriers (−11.3 to −37.9 eu) around neutral pH, with the distal Arg38 acting as an "entropic gate keeper". Dramatic enthalpy−entropy compensation is observed for BHA and 2-naphthohydroxamic acid binding to HRPC at pH 4.0. The enthalpic loss and entropic gain are likely due to increased flexibility of Arg38 in the complexes at low pH and greater access by water to the active site. Since the Soret absorption band of HRPC is a sensitive probe of the binding of hydroxamic acids and their analogues, it was used to investigate the binding of six donor substrates over the pH range of 4−12. The negligible pH dependence of the K_d values corrected for substrate ionization suggests that enthalpy−entropy compensation is operative over a wide pH range. Examination of the thermodynamics of binding of ring-substituted hyrazides to HRPC reveals that the binding affinities of aromatic donors are highly sensitive to the position and nature of the ring substituent.

Selective inhibitors have the potential to reduce toxicity caused by the generation of reactive products by peroxidases, such as hypochlorous acid production by myeloperoxidase (MPO),[1] as well as further define the activities of specific peroxidases in vivo. The design of a tight-binding peroxidase inhibitor is complicated by the observation that the majority of peroxidase−substrate interactions are weak, with K_d values in the millimolar range (*1*). A notable exception is the comparatively tight binding to horseradish peroxidase isoenzyme C (HRPC) of aromatic hydroxamic acids, which exhibit K_d values in the micromolar range (*2*). The HRPC complex with benzhydroxamic acid (BHA; $K_d = 2.4\ \mu$M) (*2*) has been studied extensively, and the H-bonds made by BHA in the distal heme cavity are the subject of much debate. The distal His42 was first implicated because of NMR NOE connectivities between it and BHA (*3*−*8*). In contrast, computer modeling of the HRPC−BHA complex suggested that the BHA side chain H-bonded exclusively to Arg38 (*9*), but this was not supported by the low affinity of both His42 and Arg38 mutants [$K_d = 2.9$ (H42L), 6.8 (H42R), 10.4 (R38G), and >12 mM (R38L)] for BHA (*10*). A role for both distal residues in BHA binding was confirmed from the HRPC−BHA crystal structure (*11*), which revealed that BHA is involved in five H-bonds in the distal cavity of HRPC: BHA CO···Arg38 $N_{\eta 2}$ (2.91 Å), BHA CO···H_2O (2.57 Å), BHA NH···Pro139 CO (2.70 Å), BHA OH···His42 $N_{\epsilon 2}$ (2.82 Å), and BHA OH···H_2O (3.12 Å). Similar H-bonds were observed in the BHA complex of *Arthromyces ramosus* peroxidase (ARP) (*12*). This is not surprising since the distal catalytic residues are highly conserved among peroxidases

† This research was supported in part by a grant from the Natural Engineering and Research Council of Canada (NSERC) to A.M.E. and MRC/PMAC Health Program and NSERC Studentships to S.M.A.

* To whom correspondence should be addressed. E-mail: english@vax2.concordia.ca. Telephone: (514) 848-3338. Fax: (514) 848-2868.

‡ Concordia University.

§ Merck Frosst Centre for Therapeutic Research.

[1] Abbreviations: ARP, *A. ramosus* peroxidase; BHA, benzhydroxamic acid; BZA, benzamide; BZH, benzhydrazide; CAPS, 3-(cyclohexylamino)-1-propanesulfonic acid; CCP, cytochrome *c* peroxidase; 2′-HA, 2′-hydroxyacetophenone; HEPES, *N*-(2-hydroxyethyl)piperazine-*N*′-2-ethanesulfonic acid; HRPC, horseradish peroxidase isoenzyme C; INH, isonicotinic hydrazide; ITC, isothermal titration calorimetry; MOPS, 3-(*N*-morpholino)propanesulfonic acid; MPO, myeloperoxidase; 2-NHA, 2-naphthohydroxamic acid; N-BH, *N*-benzylhydroxylamine; NICH, nicotinic hydrazide; NMBZA, *N*-methylbenzamide; 2-NZH, 2-naphthohydrazide; PIPES, piperazine-*N*,*N*′-bis(2-ethanesuflonic acid); SHA, salicylhydroxamic acid; TAPS, 3-{[tris(hydroxymethyl)methyl]-amino}propanesulfonic acid.

10.1021/bi010445f CCC: $20.00 © 2001 American Chemical Society
Published on Web 10/27/2001

(*13*). Structural data also reveal that the related compound, salicylhydroxamic acid (SHA), binds to ARP (*14*) and myeloperoxidase (MPO) (*15*) in a fashion similar to that of BHA in its peroxidase complexes.

The contributions of specific H-bonds to protein−substrate binding affinities are unpredictable (*16*). Also, desolvation, nonpolar interactions, and flexibility are crucial factors contributing to substrate binding energies that are sometimes overlooked since they are not as easily visualized as H-bonds (*16*). Thus, knowledge of the binding thermodynamics is key to understanding the relative contributions of the various interactions in protein−substrate complexes. A comparison of the thermodynamics of BHA binding to a series of HRPC mutants the thermodynamics of binding of a series of BHA analogues to wild-type HRPC is required to deconvolve the binding energy into the various H-bonding and nonpolar interactions identified in the HRPC−BHA complex (*11*). An advantage of the latter approach is that there is no risk of structural changes in the protein. Examples of such investigations include the thermodynamics of complex formation between pyridine nucleotide substrates and dihydrodipicolinate reductase (*17*), and the binding of phosphonamide-, phosphonate-, and phosphinate-containing inhibitors to thermolysin (*18*).

Despite extensive spectroscopic characterization, little information exists about the thermodynamics of substrate binding to heme peroxidases. Binding of BHA ($\Delta H^\circ = -13.9$ kcal/mol) and benzhydrazide (BZH, $\Delta H^\circ = -10.1$ kcal/mol) to HRPC at pH 7.0 was investigated using a stopped-flow calorimeter (*19*), and the enthalpies (ΔH°, in kilocalories per mole) of hydroquinone [−9.7 kcal/mol (*20*)] and resorcinol [−7.6 (*20*) and −5.9 kcal/mol (*21*)] binding to HRPC at pH 6.0 were estimated from Arrhenius plots assuming constant ΔC_p. Isothermal titration calorimetry (ITC) yields more accurate thermodynamic parameters than Arrhenius plots since heats of binding are measured directly and the assumption of constant ΔC_p is not necessary (*22*). Thus, as a first step in the rational design of peroxidase inhibitors, the binding of a series of BHA analogues to ferric HRPC was investigated by ITC. The resultant thermodynamic parameters are discussed here in terms of the H-bonding and nonpolar interactions of the substrates in the HRPC heme cavity. Binding constants determined spectroscopically over an extended pH range (4 −12) provide insight into the effects of substrate and HRPC ionization equilibria on substrate affinity. Since HRPC is considered an archetypical peroxidase (*23*), the findings presented here should have broad applicability in the design of peroxidase inhibitors.

MATERIALS AND METHODS

Materials. Lyophilized grade I horseradish peroxidase was purchased from Roche Molecular Biochemicals. The substrates (Figure 1) were purchased from Lancaster with the exception of 3-OH-BZH and 4-OH-BZH, which were from Aldrich. 2-NHA was kindly provided by G. R. Schonbaum. All other reagents were of the highest quality available, and all reagents were used without purification.

Isothermal Titration Calorimetry. The ITC experiments were performed at 25 °C using either a MicroCal MCS or VP ultrasensitive titration calorimeter. HRPC samples for ITC were prepared by 24 h dialysis in 100 mM buffer at pH 4.0 (sodium acetate, citrate, or tartrate), pH 6.0 (sodium phosphate), or pH 7.0 (sodium phosphate, Tris, imidazole, HEPES, PIPES, or MOPS). Substrate solutions were prepared in the dialysis buffers to ensure minimal background from buffer mismatch. The dialyzed HRPC samples (2.6 μM to 1.14 mM) were added to the 1.4 mL calorimeter sample cell. Typically, 29 injections were made at 4−8 min intervals, and the heat of reaction per injection (microcalories per second) was determined by integration of the peak areas using Origin software (MicroCal). For most of the substrates that were investigated, binding was complete within the first half of the titration and the heat of dilution was determined from the baseline following completion of the titration. Binding of BZA, NMBZA, 2′-HA, N-BH, INH, and NICH was not complete within the first half of the titration due to their weak affinity for HRPC. Therefore, heats of dilution of these compounds were determined by injection of the substrate into the buffer only. In both cases, the heat of dilution was subtracted from the observed heat of binding prior to data analysis. The Origin software provided the best-fit values of ΔH°, the stoichiometry of binding (n), and the dissociation constant (K_d) from plots of heat evolved per mole of substrate injected versus the substrate/HRPC molar ratio (*22*). The Gibbs free energy of binding [$\Delta G^\circ = RT \ln(1/K_d)$] and the entropy of binding ($T\Delta S^\circ = \Delta H^\circ - \Delta G^\circ$) were calculated from the experimental values.

Optical Titrations. Stock solutions of ferric HRPC in 100 mM sodium phosphate (pH 7.0) were diluted into the following buffers (all 100 mM): sodium tartrate (pH 4.0), sodium acetate (pH 5.0), sodium phosphate (pH 6.0, 7.0, 8.0, and 12.0), TAPS (pH 9.0), and CAPS (pH 10.0). Stock solutions (100 mM) of the substrates were prepared by weight in DMSO and serial dilutions made into the appropriate buffer. Protein−substrate optical titrations were performed by the successive addition of 2 μL aliquots of substrate at the appropriate concentration to 2.5 μM ferric HRPC in 3 mL quartz cuvettes. Samples were mixed with a magnetic stirbar and allowed to equilibrate for 15 min at 25 °C before the UV−vis spectra were recorded. Titrations with BZH at pH 7.0 were carried out under N_2 in sealed cuvettes. The observed or apparent dissociation constants [$K_{d(app)}$] were determined from least-squares fits of eq 1:

$$[E\cdot S] = \frac{[E]_T[S]}{K_{d(app)} + [S]} \quad (1)$$

where $[E]_T$ is the total enzyme concentration, [E·S] the concentration of bound substrate [$[E\cdot S] = \Delta A/\Delta\epsilon$, where ΔA is the absorbance difference between the free enzyme (E) and the E·S complex and $\Delta\epsilon$ the corresponding difference in molar absorptivity], and [S] the concentration of free substrate ($[S] = [S]_T - [E\cdot S]$ or $[S] = [S]_T$ for $[S]_T \gg [E]_T$) (*24*). $K_{d(app)}$ values were corrected for substrate ionization [$K_d = \alpha K_{d(app)}$] by multiplying by α, the fraction of the unionized substrate.

RESULTS

The structures of the aromatic substrates used are shown in Figure 1 and representative calorimetric titrations at pH

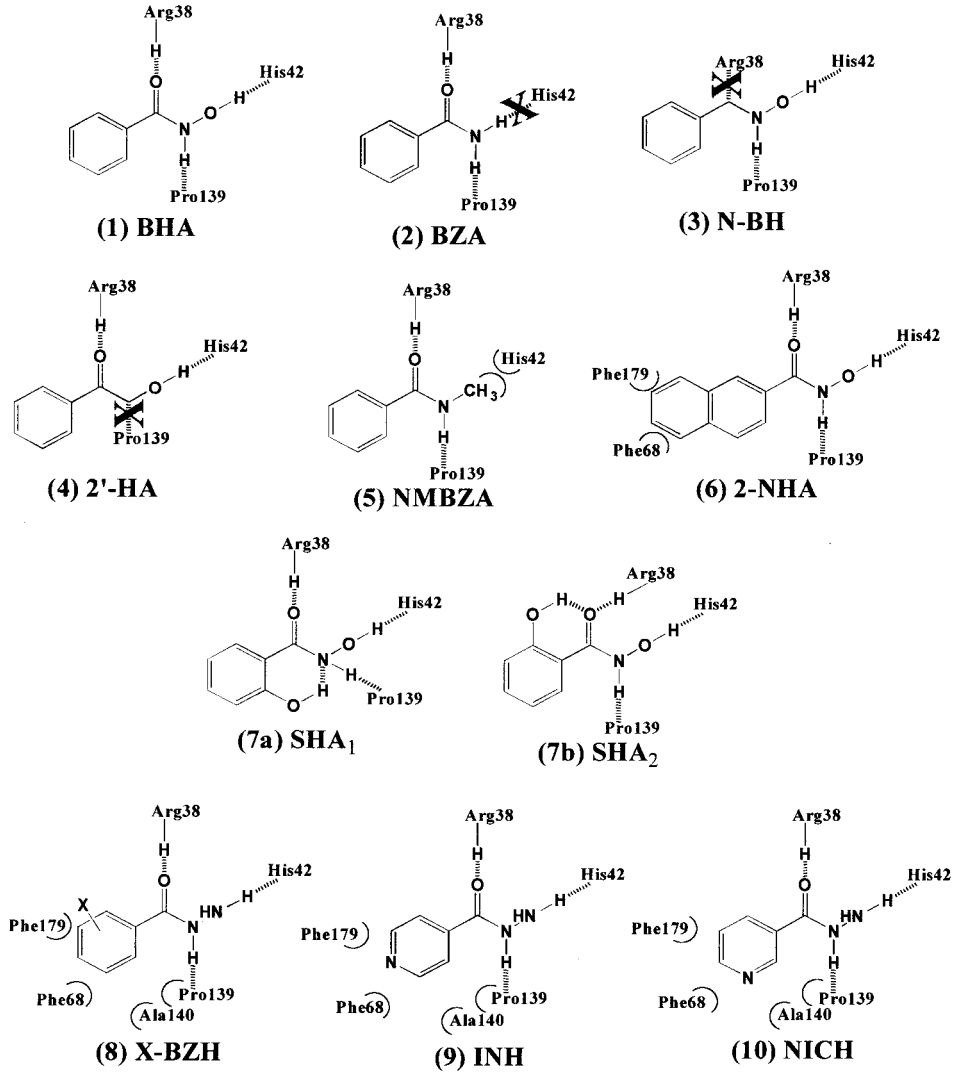

FIGURE 1: Structures of the aromatic substrates used in the HRPC binding studies. The H-bonds (hashed lines) between the substrates and residues in the distal cavity of HRPC are based on the HRPC−BHA crystal structure (*11*) except those shown for the SHA_1 and SHA_2 conformers, which are based on the MPO−SHA (*15*) and ARP−SHA crystal structures (*14*), respectively. Key hydrophobic contacts or steric interactions (semicircles) are shown only for substrates with a naphthyl ring (2-NHA and 2-NZH) or a substituted phenyl ring, and for the methyl group of NMBZA. Unsubstituted phenyl rings are assumed to make the same hydrophobic contacts as that of BHA in its HRPC complex (*11*). Substrates: (1) benzhydroxamic acid (BHA), (2) benzamide (BZA), (3) *N*-benzylhydroxylamine (N-BH), (4) 2′-hydroxyacetophenone (2′-HA), (5) *N*-methylbenzamide (NMBZA), (6) 2-naphthohydroxamic acid (2-NHA), (7a,b) salicylhydroxamic acid (SHA), (8) X-BZH, where X is H [benzhydrazide (BZH)], phenyl [2-naphthohydrazide (2-NZH)], and *ortho*, *meta*, or *para* OH, CH_3, Cl, NH_2, or NO_2, (9) isonicotinic hydrazide (INH), and (10) nicotinic hydrazide (NICH).

7.0 of HRPC with BHA and NMBZA in Figure 2. Each peak in the binding isotherm (top panels, Figure 2) represents a single injection of substrate, and the negative deflections from the baseline indicate that heat was evolved. The enthalpy change on each injection was plotted versus the substrate/HRPC molar ratio (bottom panels, Figure 2), and n, $\Delta H°$, K_d, $\Delta G°$, and $\Delta S°$ were determined from the plots. The shape of the titration curve depends on c ($[HRP]_T/K_d$) (*22*) and is rectangular for high c values (>100) and flat for low c values (<0.1). Less accurate K_d values are obtained outside the desired range (5−50) of c values. The K_d of 2.5 μM [Table 1 (*2*)] for BHA is ideal for ITC, requiring a $[HRP]_T$ of ∼12.5−25 μM for a c of ∼5−50 (note that $[HRP]_T = 33$ μM and $c = 13$ in Figure 2A). However, to attain c values within the desired range for NMBZA ($K_d = 410$ μM, Table 1), prohibitively high $[HRP]_T$ values (2−20 mM) would be required. The $[HRP]_T$ that was used (0.21 mM; $c = 0.6$) resulted in a shallow titration curve for NMBZA (Figure 2B), which is typical of the curves obtained for substrates with millimolar K_d values.

Contribution of Buffer Ionization to the Observed Enthalpy of Binding. The binding enthalpy measured by ITC ($\Delta H°_{obs}$) contains contributions from the buffer ionization enthalpy ($\Delta H°_{buffer}$) according to (*25*)

$$\Delta H°_{obs} = \Delta H°_{bind} + n_{H^+}\Delta H°_{buffer} \quad (2)$$

where $\Delta H°_{bind}$ is the buffer-independent binding enthalpy and n_{H^+} the number of protons taken up or released during the binding process. Plots of $\Delta H°_{obs}$ versus $\Delta H°_{buffer}$ for BHA, SHA, and 2-NHA binding to HRPC in six buffers at pH 7.0 are shown in Figure 3. The positive n_{H^+} values reveal the uptake of 0.28 ± 0.032, 0.13 ± 0.034, and 0.22 ± 0.026 proton by the BHA, SHA, and 2-NHA complexes, respectively. The $\Delta H°_{bind}$ values of −14.4 ± 0.21, −15.3 ± 0.23, and −15.0 ± 0.19 kcal/mol for BHA, SHA, and 2-NHA,

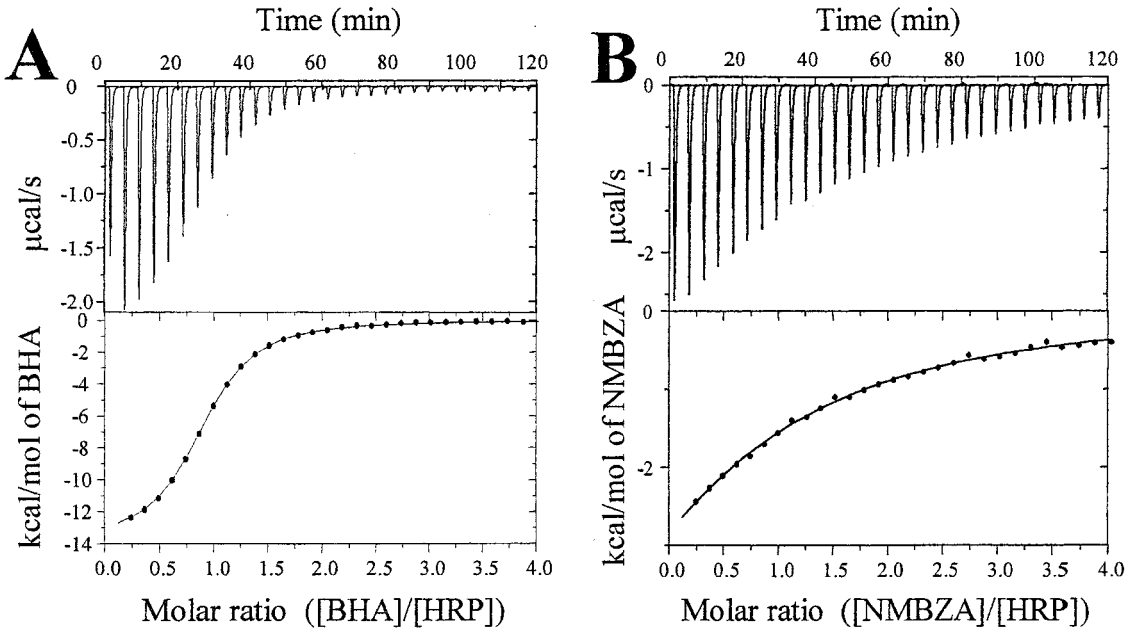

FIGURE 2: Isothermal calorimetry titration of (A) 33 μM HRPC with 560 μM BHA and (B) 0.21 mM HRPC with 3.52 mM NMBZA in 100 mM sodium phosphate buffer at pH 7.0 and 25 °C. In the top panels, the heat released per unit time (microcalories per second) is plotted vs time where each peak corresponds to the injection of an aliquot of substrate. In the bottom panels, the heat of reaction per injection (kilocalories per mole of substrate) was determined by integration of the area under each peak, plotted vs [substrate]/[HRPC], and fit using the software provided by MicroCal.

Table 1: Dissociation Constants and Thermodynamic Data for Binding of Aromatic Hydroxamic Acid Analogues to Ferric HRPC

compd	pH[a]	K_d (μM) (spec)[b]	K_d (μM) (ITC)[a]	n[c]	$\Delta G°$ (kcal/mol)[d]	$\Delta H°$ (kcal/mol)[a]	$\Delta S°$ (eu)[e]
BZA	7	2700 ± 50	4300 ± 91	0.75 ± 0.07	−3.23	−9.52 ± 0.98	−21.1
NMBZA	7	410 ± 2	360 ± 29	0.85 ± 0.11	−4.70	−8.22 ± 1.22	−11.8
2′-HA	7	~2000	13000 ± 184	0.85 ± 0	−2.57	−8.68 ± 0.31	−20.5
N-BH	7	nd[f]	19000 ± 2000	0.85 ± 0	−2.35	−7.40 ± 0.14	−16.9
BHA	4	6.4 ± 0.04	7.3 ± 1.0	0.86 ± 0.19	−7.00	−9.20	−6.71
BHA	7	2.5 ± 0.01	2.5 ± 0.05	0.90 ± 0.003	−7.64	−14.1 ± 0.07	−21.8
SHA	7	11 ± 0.1	12 ± 0.4	0.90 ± 0.007	−6.69	−15.5 ± 0.16	−29.4
2-NHA	4	0.40 ± 0.01	0.60 ± 0.13	0.94 ± 0.10	−8.48	−10.0	−5.10
2-NHA	7	0.15 ± 0.01	0.16 ± 0.04	1.0 ± 0.04	−9.27	−14.8 ± 0.94	−18.4

[a] Experiments at pH 4.0 were conducted in 100 mM tartrate, citrate, and acetate buffers, and the mean K_d (ITC) values are given. The pH 4.0 $\Delta H°$ values were corrected for buffer ionization using eq 2. The pH 6.0 and 7.0 $\Delta H°$ values are those measured in 100 mM sodium phosphate (see the text). [b] Spectroscopically determined K_d values from Table 2. [c] The stoichiometry of binding determined by ITC. [d] $\Delta G°$ from K_d (ITC). [e] eu, entropy units (calories per mole per kelvin). [f] Not determined.

respectively, are within experimental error of the $\Delta H°_{obs}$ values in 100 mM sodium phosphate at pH 7.0 (−14.1 ± 0.07, −15.5 ± 0.07, and −14.8 ± 0.9 kcal/mol). Hence, it is assumed that in phosphate buffer at pH 7.0 $\Delta H°_{obs}$ (which is abbreviated to $\Delta H°$ from this point forward) is equal to $\Delta H°_{bind}$ for the aromatic hydroxamic acids. The contribution of $n_{H^+}\Delta H°_{buffer}$ to $\Delta H°_{obs}$ is also expected to be small for the other substrates in Figure 1 since they do not ionize around pH 7.0.

$\Delta H°$ was measured in three buffers at pH 4.0 (sodium tartrate, $\Delta H°_{buffer} = -0.76$ kcal/mol; sodium acetate, $\Delta H°_{buffer} = -0.10$ kcal/mol; and sodium citrate, $\Delta H°_{buffer} = 0.58$ kcal/mol) (*26*). Plots of $\Delta H°_{obs}$ versus $\Delta H°_{buffer}$ (data not shown) yielded n_{H^+} values of 0.57 ± 0.011 and 0.98 ± 0.234 for BHA and 2-NHA, respectively, indicating uptake of ~1 proton by their HRPC complexes at pH 4.0. Given the range of $n_{H^+}\Delta H°_{buffer}$ values (from −0.43 to 0.33 kcal/mol for BHA and from −0.74 to 0.57 kcal/mol for 2-NHA), the pH 4.0 $\Delta H°$ values in Table 1 (−9.20 and −10.0 kcal/mol) were corrected for buffer ionization.

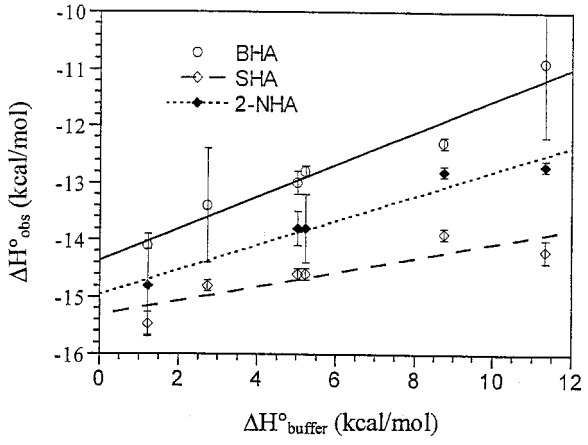

FIGURE 3: Plot of $\Delta H°_{obs}$ vs $\Delta H°_{buffer}$ for BHA, SHA, and 2-NHA in 100 mM buffer at pH 7.0 and 25 °C. The buffers used and their $\Delta H°_{buffer}$ values at 25 °C are as follows: 1.22 kcal/mol for sodium phosphate, 2.74 kcal/mol for PIPES, 5.02 kcal/mol for HEPES, 5.22 kcal/mol for MOPS, 8.75 kcal/mol for imidazole, and 11.34 kcal/mol for Tris (*48*). Values of n_{H^+} and $\Delta H°_{bind}$ were determined from fits of the data to eq 2 (see the text).

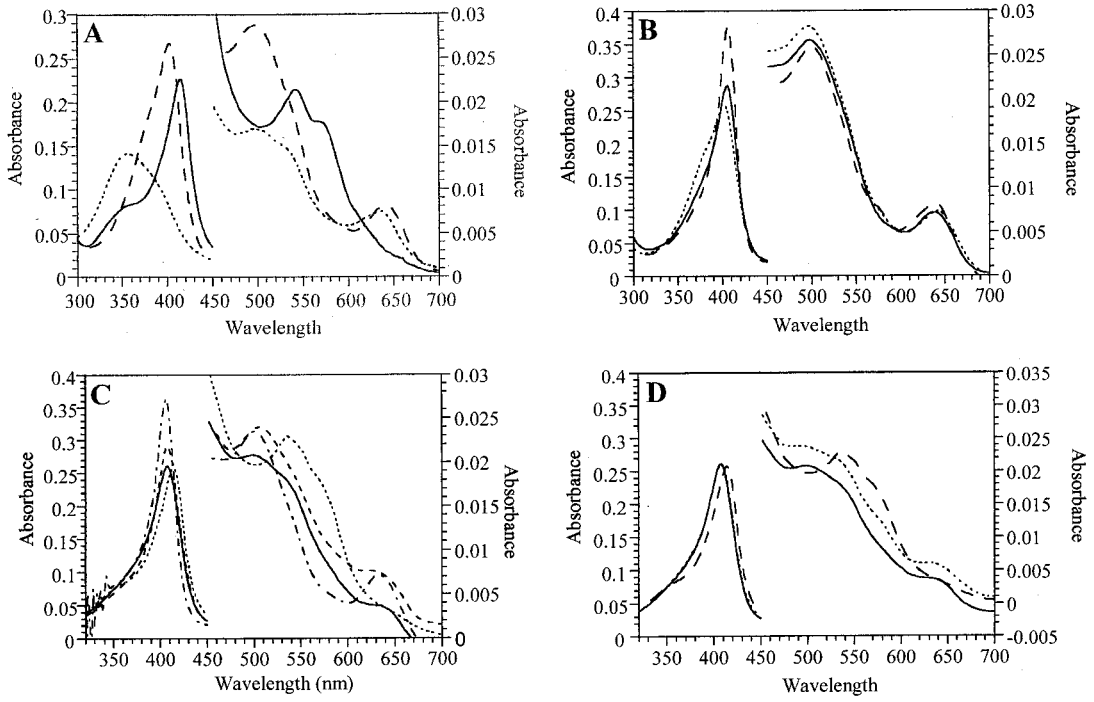

FIGURE 4: (A) Absorption spectra of 2.5 μM ferric HRPC at pH 3.0−12.0. HRPC was equilibrated for 15 min in 100 mM buffer at pH 3.0 (···) (sodium tartrate) and at pH 7.0 (− − −) and 12.0 (—) (sodium phosphate) prior to spectral acquisition. (B) Effect of substrate binding on the Soret absorption of 2.5 μM ferric HRPC in 100 mM sodium phosphate at pH 7.0: free HRPC (···) and HRPC in the presence of 25 mM BHA (− − −) and BZA (—). (C) Effect of substrate binding on the Soret absorption of 2.5 μM ferric HRPC in 100 mM sodium phosphate at pH 12.0: free HRPC (···) and HRPC in the presence of 25 mM BHA (−·−), BZA (—), and NMBZA (− − −). (D) Observed (—) and calculated spectra (···) for 2.5 μM ferric HRPC−BZA complex at pH 12.0 assuming a p$K_{a(app)}$ of 11.9 (eq 3) for the alkaline transition of HRPC in the presence of 25 mM BZA. The spectrum of 2.5 μM free ferric HRPC at pH 12.0 (− − −) is shown for comparison.

Thermodynamic Parameters for Binding of Aromatic Hydroxamic Acid Analogues to HRPC at pH 7.0 and 4.0. Table 1 summarizes the binding parameters for compounds **1**−**7** in Figure 1. N-BH, 2′-HA, and BZA, which lack the hydroxamic acid CO, NH, and OH groups, respectively (Figure 1), bind to HRPC 10^3−10^4-fold less tightly than BHA at pH 7.0 (Table 1). The lower affinity of HRPC for the analogues is clearly enthalpic in origin since the $\Delta S°$ values are more positive. In contrast, the binding of SHA, which has the potential to form one extra H-bond compared to BHA, is enthalpically more favorable but entropically much less favorable than BHA binding. The enthalpic and entropic gains for 2-NHA relative to BHA binding are likely due to desolvation of the additional aromatic ring. Similarly, the entropically driven tighter binding of NMBZA, compared to that of BZA, is partly attributed to desolvation of the NMBZA methyl group on complexation.

Both BHA and 2-NHA binding at pH 4.0 [which is close to the pK_a of the distal His42 in ferric HRPC (*27*)] is enthalpically less favorable by 4.9 and 4.8 kcal/mol, respectively, than at pH 7.0 (Table 1). Nonetheless, the binding energies are only slightly lower at the lower pH due to the large entropic compensation ($T\Delta\Delta S°$, in kilocalories per mole) of 4.5 (BHA) and 4.0 (2-NHA).

Optical Titrations of Substrate Binding to Ferric HRPC at pH 4−*12.* Optical titrations over an extended pH range were carried out for substrates whose binding to HRPC is not spectroscopically silent. The Soret absorption of free ferric HRPC did not change appreciably over 15 min at pH 4.0−10.0, and the spectra resemble that shown in Figure 4A at pH 7.0. At pH 3.0, the Soret band broadened significantly and shifted to 368 nm within ∼10 min (data not shown), which is indicative of a solvent-exposed heme (*28*). The Soret shift to 416 nm at pH 12.0, in combination with the appearance of bands at 543 and 575 nm (Figure 4A), is attributed to the alkaline transition (pK_a = 10.9) of HRPC (*29*), which results in OH^- ligation to form six-coordinate low-spin Fe^{III} (*30*, *31*).

As previously observed (*2*), the binding of BHA to HRPC causes the Soret band to intensify and red-shift, with smaller changes occurring on binding of the other substrates such as BZA (Figure 4B). Also, the alkaline transition of ferric HRPC is depressed to a greater extent in the presence of BHA than in the presence of BZA or NMBZA, as predicted from eq 3 (*2*):

$$pK_{a(app)} = 10.9 + \log\left(1 + \frac{[S]_T}{K_d}\right) \qquad (3)$$

where p$K_{a(app)}$ is the expected pH value at the alkaline transition midpoint of HRPC in the presence of $[S]_T$ and K_d the dissociation constant for the HRPC·S complex at pH 7.0. From the K_d values in Tables 1 and 2, the expected p$K_{a(app)}$ values are 15.0, 12.7, and 11.9 in the presence of 25 mM BHA, NMBZA, and BZA, respectively. As predicted, the pH 12.0 spectra of the HRPC−BHA and HRPC−NMBZA complexes (Figure 4C) are similar to those at pH 7.0, while the spectrum in the presence of 25 mM BZA can be fit by a sum of the HRPC−BZA pH 7.0 spectrum and the free HRPC pH 12.0 spectrum (Figure 4D). Bands appeared at 543 and 575 nm in the spectra of ferric HRPC upon addition of BZH under aerobic conditions at pH ≥7 due to oxyHRPC ($Fe^{II}O_2$) formation (S. Aitken, unpublished results). However, in the absence of O_2, the HRPC−BZH spectrum (not shown)

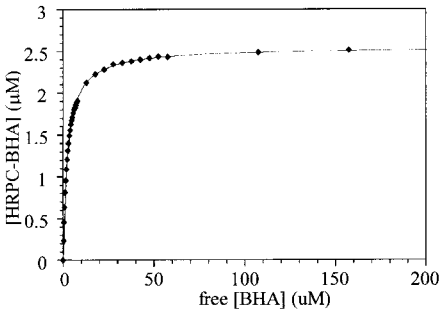

FIGURE 5: Optical titration of 2.5 μM ferric HRPC with BHA at pH 7.0. HRPC was equilibrated for 15 min in 100 mM sodium phosphate buffer at 25 °C prior to titration with BHA. The concentration of the HRPC−BHA complex was determined from $\Delta A/\Delta\epsilon$ at 406 nm ($\Delta\epsilon_{406}$ = 49 mM^{-1} cm^{-1}) for free HRPC and the HRPC−BHA complex, and the free BHA concentration was determined by subtracting the concentration of the HRPC−BHA complex from the total BHA concentration.

is similar to the HRPC−BHA spectrum (Figure 4B). A stable spectrum was not obtained for the HRPC−BZH complex at pH 12.0 because of the sensitivity of the sample to trace amounts of O_2 in the N_2-purged cuvette.

A representative optical titration of HRPC with BHA at pH 7.0 is shown in Figure 5, and the apparent dissociation constants, $K_{d(app)}$, from the titration of HRPC with six substrates over the pH range of 4−12 are summarized in Table 2. Without exception, the $K_{d(app)}$ values increase slightly (∼2−7-fold) at pH 4.0, which is assigned to changes in the protein (*27*), since the substrates do not ionize over the pH range of 4−7 (*2*). In contrast, the decreased affinity of HRPC for the hydroxamic acids at pH >7.0 (Table 2) can be attributed to their ionization since the anions reportedly do not bind to HRPC (*2*). When the fraction of un-ionized substrate (α_{HA}) is taken into account, the BHA K_d [=$\alpha_{HA}K_{d(app)}$] shows little variation over the pH range of 4−12 (Table 3). The corrected K_d values for 2-NHA, calculated using the reported pK_a of 7.7 (*32*), decrease significantly with increasing pH, but not when the BHA pK_a of 8.8 (*2*) is assumed (Table 3), suggesting that the pK_a values for the two hydroxamic acids are similar, as expected.

Free SHA exhibits pK_a values at 7.4 and 10.0 (Figure 6). The former value agrees with the literature pK_a of 7.43 for the hydroxamic acid group (*32*), and a pK_a of 10.0 is assigned to the ring hydroxyl, which is close to the value of 9.95 for phenol. The K_d values [$\alpha_{H_2A}K_{d(app)}$] for binding of only the neutral form (H_2A) of SHA to HRPC showed little variation with pH (Table 3), but the values [$(\alpha_{HA^-} + \alpha_{H_2A})K_{d(app)}$] for both H_2A and HA^- binding increased significantly at alkaline pH (Table 3), indicating that only the neutral form of SHA binds to HRPC. The corrected K_d values are lowest at high pH (Table 3), and the increased substrate affinity is attributed to changes in HRPC other than those induced by the heme-linked alkaline transition.

Effects of Ring Substituents on the Binding of Hydrazides to HRPC at pH 6.0. These studies were performed at pH 6.0 since oxyHRPC is formed under aerobic conditions at higher pHs in the presence of hydrazides (S. Aitken, unpublished results). The binding of 19 hydrazides (Figure 1) to ferric HRPC was investigated, and their thermodynamic binding parameters are summarized in Table 4. Using BZH as the reference hydrazide, the effects of the ring substituents on binding affinities are presented graphically in Figure 7. The range of values obtained ($\Delta\Delta H° = \Delta H°_{substrate} - \Delta H°_{BZH}$ = −4.00 to 3.53 kcal/mol, and $T\Delta\Delta S° = T\Delta S°_{substrate} - T\Delta S°_{BZH}$ = −4.92 to 3.01 kcal/mol with 2-OH-BZH and 4-Cl-BZH values at the extremes) reveals that the complexation equilibria between HRPC and aromatic substrates are highly sensitive to the position and nature of the ring substituent.

DISCUSSION

H-Bonding in the Distal Heme Cavity of Ferric HRPC. Substrates **2**−**4** (Figure 1) each lack one of the three H-bonding atoms of the BHA side chain (*11*). In water, a charged H-bond can contribute as much as 8.3 and 4.7 kcal/mol, respectively, to the $\Delta H°$ and $\Delta G°$ values of substrate binding, while the corresponding contributions of a neutral H-bond are 1.9−3.0 and 0.5−1.5 kcal/mol, respectively (*16*, *33*−*36*). The $\Delta\Delta H°$ and $\Delta\Delta G°$ of 6.7 and 5.29 kcal/mol, respectively, for N-BH relative to BHA (Table 1) reflect the absence of the charged H-bond, CO···Arg38, as well as the neutral H-bond, CO···H_2O. The K_d values for the R38G (10.4 mM) and R38L (>12 mM) mutants for BHA (*10*) are close in value to the K_d for wild-type HRPC for N-BH (19 mM, Table 1). The $\Delta\Delta H°$ and $\Delta\Delta G°$ values of 4.62 and 4.41 kcal/mol, respectively, for BZA relative to BHA (Table 1) fall within the values expected for the loss of the two neutral H-bonds, OH···His42 and OH···H_2O (*11*). Again, the K_d values of the H42L (2.9 mM) and H42R (6.8 mM) mutants for BHA are very similar to the K_d of wild-type HRPC for BZA (4.3 mM, Table 1). The $\Delta\Delta H°$ and $\Delta\Delta G°$ values of 5.4 and 5.07 kcal/mol, respectively (Table 1), for the binding of 2′-HA relative to that of BHA are greater than expected for the loss of a single, neutral H-bond (NH···Pro139). However, 2′-HA (pK_a > 15) is a poorer H-bond donor than BHA (pK_a = 8.8), which will significantly weaken the OH··· His42 H-bond in the 2′-HA complex. The effect of substrate pK_a is also seen in the $\Delta\Delta H°$ (−3.3 kcal/mol) and $\Delta\Delta G°$ (−2.24 kcal/mol) values for BHA compared to those for BZH [pK_a ∼ 12 (*2*)] binding to HRPC at pH 6.0 (Table 4), which confirms that a good H-bond donor is required to form a strong H-bond to the distal His42.

The large negative $\Delta S°$ values in Table 1 reveal that the low substrate binding affinities of HRPC are entropically derived at pH 7.0. This provides HRPC with built-in "entropic" protection from the highly reactive, one-electron-oxidized forms of its donors. With the notable exception of the CO···Arg38 interaction, the absence of H-bonds between HRPC and the side chains of the BHA analogues at pH 7.0 has little entropic consequence [$\Delta S°$, BHA (−21.8 eu) > BZA (−21.1 eu) > 2′-HA (−20.5 eu) > N-BH (−16.9)]. The $\Delta\Delta S°$ of ∼5 eu for N-BH versus BHA is attributed to the increased flexibility of the distal Arg38 in the N-BH complex (Figure 1) since the distal arginine is reported to be highly flexible in heme peroxidases. For example, the distal Arg48 of CCP moves ∼3 Å to interact with heme-bound ligands (*37*).

Arg38 flexibility may also be implicated in the >4-fold lower affinity of HRPC for SHA versus BHA despite the enthalpic gain ($\Delta\Delta H° = -1.33$ kcal/mol) from the low pK_a (=7.4; Figure 6) of the SHA hydroxamate OH plus the additional H-bond formed by the ring 2-OH. Figure 1 shows two possible conformers of HRPC-bound SHA. Conformer

Table 2: pH Dependence of the Apparent Dissociation Constants, $K_{d(app)}$ (Micromolar), for Binding of Aromatic Hydroxamic Analogues to Ferric HRPC

pH	BZH[a]	BZA[b]	NMBZA	BHA	SHA	2-NHA
4.0	362 ± 5	5.4 ± 0.1	(2.8 ± 0.02) × 10^3	6.4 ± 0.04	18 ± 0.1	0.40 ± 0.01
5.0	154 ± 5	3.8 ± 0.1	595 ± 6	3.3 ± 0.02	9.2 ± 0.1	0.24 ± 0.01
6.0	109 ± 2	2.6 ± 0.05	376 ± 3	2.3 ± 0.01	7.7 ± 0.04	0.16 ± 0.004
7.0	90 ± 2	2.7 ± 0.05	411 ± 2	2.5 ± 0.01	11 ± 0.1	0.15 ± 0.01
8.0	85 ± 2	2.8 ± 0.06	400 ± 2	2.8 ± 0.01	30 ± 0.1	0.22 ± 0.006
9.0	83 ± 1	2.8 ± 0.04	359 ± 2	21 ± 1	313 ± 15	1.1 ± 0.1
10.0	204 ± 12	(3.3 ± 0.04) × 10^3	301 ± 1	174 ± 3	(1.1 ± 0.1) × 10^3	2.0 ± 0.03
12.0		(9.2 ± 0.4) × 10^3	(2.0 ± 0.05) × 10^3	(2.1 ± 0.3) × 10^3		387 ± 21

[a] The $K_{d(app)}$ values were determined under anaerobic conditions since the HRPC−BZH complex exhibits time-dependent spectra in air (see the text). [b] $K_{d(app)}$ values for BZA only are in millimolar.

Table 3: Dissociation Constants, K_d (Micromolar), Corrected for Substrate Ionization for Binding of Aromatic Hydroxamic Acids to Ferric HRPC at pH 4−12[a]

pH	BHA[b]	SHA[c]	SHA^- + SHA[d]	2-NHA[e]	2-NHA[f]
4.0	6.4	18	18	0.38	0.39
5.0	3.3	9.2	9.2	0.24	0.24
6.0	2.3	7.4	7.7	0.16	0.16
7.0	2.5	7.9	11	0.15	0.13
8.0	2.4	6.0	30	0.19	7.2 × 10^{-2}
9.0	8.0	7.0	285	0.42	5.2 × 10^{-2}
10.0	10.4	1.3	531	0.12	1.0 × 10^{-2}
12.0	1.2			0.23	1.9 × 10^{-2}

[a] $K_d = \alpha K_{d(app)}$, where α is the fraction of hydroxamic acid in the neutral form and $K_{d(app)}$ the apparent dissociation constant from Table 2. [b] K_d assuming a pK_a of 8.8 for BHA (*2*). [c] K_d assuming only the neutral form of SHA binds to HRPC and pK_{a1} = 7.4 for SHA. [d] K_d assuming both neutral and singly ionized forms of SHA bind to HRPC, and pK_{a1} = 7.4 and pK_{a2} = 10.0 for SHA. [e] K_d assuming pK_a = 8.8 for NHA (see the text). [f] K_d assuming pK_a = 7.7 for NHA (see the text).

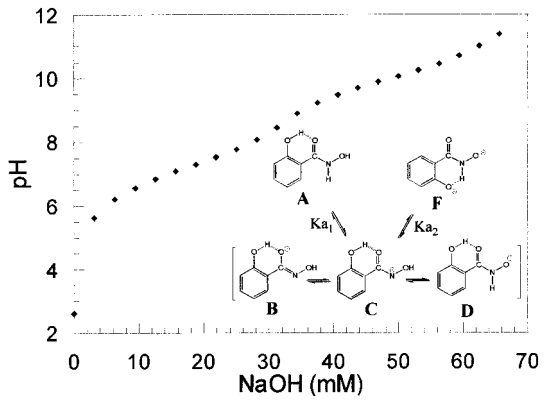

FIGURE 6: pH titration of 40 mM SHA vs 1.0 M NaOH. The pK_{a1} and pK_{a2} values were determined separately by fitting the data points for the titration of each proton to the equation $y = (a - b)/[1 + ([\mathrm{NaOH}]/\mathrm{p}K_a)^c] + b$, where y is the pH, a is the pH as [NaOH] → ∞, b is the pH as [NaOH] → 0, and c is the slope when pH = pK_a. The tautomeric forms of neutral and singly ionized SHA are also shown.

SHA_1, modeled on the MPO−SHA X-ray structure (*15*), is unlikely due to steric repulsion between the ring 2-OH and the carbonyl of Pro139. In conformer SHA_2, based on the ARP−SHA X-ray structure (*14*), the 2-OH group is within H-bonding distance of Arg38. H-Bonding to both the ring 2-OH and the hydroxamate CO should result in a more constrained conformation for Arg38, consistent with the $\Delta\Delta S°$ of −7.6 eu for SHA versus BHA binding (Table 1). Desolvation of the 2-OH group is also expected to contribute to the highly unfavorable $\Delta S°$ for SHA binding, but intramolecular H-bonding in free SHA (*14*, *15*, *38*) should offset this by attenuating the change in substrate flexibility on complexation to HRPC.

BHA and 2-NHA bind only 3- and 4-fold less tightly to the acid conformation of HRPC due to entropy−enthalpy compensation relative to the pH 7.0 values (Table 1). The large positive increments in $\Delta H°$ and $\Delta S°$ for both BHA (4.9 kcal/mol and 15.9 eu, respectively) and NHA (4.8 kcal/mol and 13.3 eu, respectively) binding at pH 4.0 versus binding at pH 7.0 suggest weakening or loss of the hydroxamate CO···Arg38 H-bond. This is consistent with the results of a pH titration of the C−O stretching vibrations of the Fe^{II}-bound CO ligand in the HRPC−CO−BHA ternary complex, which indicated that H-bonding between the distal Arg38 and the CO ligand was eliminated at low pH (*27*). Clearly, the distal Arg38 adopts different conformations at pH 7.0 and 4.0.

Another factor to consider is the proton uptake by the HRPC−BHA (n_{H^+} = 0.57) and HRPC−2-NHA (n_{H^+} = 0.98) complexes, which was revealed by a linear least-squares fit of the pH 4.0 thermodynamic data to eq 2 (vide supra). If we assume that the distal His42, which has a pK_a of ∼4 in free ferric HRPC (*27*), is the site of protonation in the complexes, then it would not accept an H-bond from BHA or 2-NHA (Figure 1) at pH 4.0. Interestingly, a pK_a of 4.5 was proposed for His42 in the HRPC−CO complex (*27*), but this assignment is questionable since the HRPC(H42L)−CO complex exhibited a similar pK_a (*39*). $\Delta H°_{bind}$ in eq 2 is composed of a term that is independent of the protonation event ($\Delta H°'$) and a term that describes the contribution of protonation to the enthalpy change (*25*):

$$\Delta H°_{bind} = \Delta H°' + n_{H^+}\Delta H°_{prot} \quad (4)$$

Since $\Delta H°_{prot}$ = −6.28 kcal/mol for an imidazole group (*40*), protonation of His42 on complexation would yield an $n_{H^+}\Delta H°_{prot}$ value of −3.58 kcal/mol and a $\Delta H°'$ of −5.62 kcal/mol for the HRPC−BHA complex at pH 4.0; the corresponding values for 2-NHA would be −6.15 kcal/mol ($n_{H^+}\Delta H°_{prot}$) and −3.85 kcal/mol ($\Delta H°'$). On the other hand, if Asp43 or one of the heme propionates is protonated, $\Delta H°_{bind} = \Delta H°'$ since $\Delta H°_{prot} \sim 0$ kcal/mol for a carboxylate group (*40*). To determine $\Delta H°_{prot}$, and hence the possible site of protonation in the HRPC complexes, an investigation of substrate binding over a pH range with a constant $\Delta H°'$ is necessary (*25*).

The spectroscopic survey versus pH reveals that all the substrates in Table 2 bind to HRPC less tightly at pH 4.0 than at pH 7.0. Since NMBZA, which cannot form the OH···His48 H-bond (Figure 1), loses the most binding

Table 4: Effects of Ring Substituents on the Thermodynamics of Aromatic Hydrazide Binding to Ferric HRPC[a]

comd	K_d (μM) (spec)[b]	K_d (μM) (ITC)	n[c]	$\Delta G°$ (kcal/mol)[c]	$\Delta H°$ (kcal/mol)	$\Delta S°$ (eu)[d]
BZH	109 ± 2	120 ± 2	0.84 ± 0.007	−5.35	−11.7 ± 0.13	−21.4
2-OH-BZH	439 ± 45	627 ± 18	0.81 ± 0.05	−4.37	−15.7 ± 1.00	−37.9
2-NH_2-BZH	2960 ± 260	3100 ± 220	0.89 ± 0	−3.42	−11.8 ± 0.6	−28.1
2-Cl-BZH	2320 ± 80	2050 ± 38	0.85 ± 0	−3.76	−9.99 ± 0.088	−21.2
2-CH_3-BZH	2300 ± 50	2760 ± 28	0.85 ± 0	−3.49	−10.2 ± 0.052	−22.6
2-NO_2-BZH	85000 ± 32000					
3-OH-BZH	87 ± 1	120 ± 1	0.85 ± 0.01	−5.35	−13.3 ± 0.11	−26.8
3-NH_2-BZH	250 ± 12	250 ± 10	0.81 ± 0.06	−4.91	−12.1 ± 1.01	−24.1
3-Cl-BZH	99 ± 4	267 ± 14	0.82 ± 0.06	−4.87	−9.78 ± 0.76	−16.4
3-CH_3-BZH	76 ± 1	108 ± 3	0.89 ± 0.01	−5.41	−10.9 ± 0.17	−18.4
3-NO_2-BZH	9110 ± 48					
4-CH_3-BZH	118 ± 7	143 ± 5	0.89 ± 0	−5.24	−11.3 ± 0.12	−20.3
4-OH-BZH	220 ± 22	540 ± 24	1.37 ± 0.05	−4.46	−8.45 ± 0.39	−13.4
4-NH_2-BZH	303 ± 11	231 ± 18	0.92 ± 0.05	−4.96	−11.1 ± 0.68	−20.7
4-Cl-BZH	135 ± 5	297 ± 9	0.85 ± 0	−4.81	−8.17 ± 0.098	−11.3
4-NO_2-BZH	3020 ± 1160					
INH	1100 ± 34	3360 ± 35	0.85 ± 0	−3.37	−8.43 ± 0.061	−17.0
NICH	4260 ± 275	4620 ± 154	0.85 ± 0	−3.18	−7.25 ± 0.14	−13.6
2-NZH	0.917 ± 0.062	5.2 ± 0.11	0.92 ± 0.005	−7.20	−14.27 ± 0.11	−23.7
BHA	2.3 ± 0.01	2.7 ± 0.1	083 ± 0.003	−7.59	−15.0 ± 0.07	−24.69

[a] All experiments were conducted in 100 mM sodium phosphate buffer at pH 6.0. [b] Spectroscopically determined K_d values. [c] The stoichiometry of binding determined by ITC, and $\Delta G°$ from K_d (ITC). [d] eu, entropy units (calories per mole per kelvin).

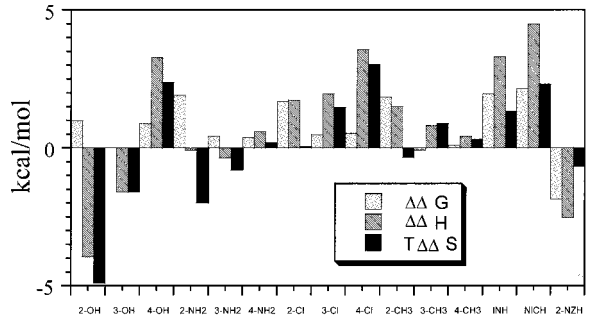

FIGURE 7: Comparison, using BZH as a reference, of the thermodynamic parameters for binding to ferric HRPC in 100 mM sodium phosphate at pH 6.0 of the ring-substituted aromatic hydrazides, including INH, NICH, and 2-NZH. $\Delta\Delta H° = \Delta H°_{substrate} - \Delta H°_{BZH} > 0$, $T\Delta\Delta S° = T\Delta S°_{substrate} - T\Delta S°_{BZH} > 0$, and $\Delta\Delta G° = \Delta G°_{substrate} - \Delta G°_{BZH} > 0$ indicate that binding of a given hydrazide to HRPC is enthalpically *less* favorable, entropically *more* favorable, and *weaker*, respectively, than binding of BZH. The thermodynamic data are from Table 4.

affinity (~7-fold) at low pH, the increased $K_{d(app)}$ values at pH 4.0 are attributed mainly to conformational changes in the distal Arg38 as discussed above. Unfortunately, the HRPC−N-BH complex is spectroscopically silent so the effects of removing the hydroxamate CO·Arg38 interaction (Figure 1) cannot be readily probed as a function of pH. Nevertheless, consistent with our interpretation of the low-pH substrate binding data, biophysical studies reveal that HRPC has a looser conformation at pH 4.0 (*41*, *42*), and in reporting on the X-ray structure, Gajhede et al. (*43*) speculated that extremes of pH would likely alter H-bonding in the distal cavity of HRPC.

Upon OH^- ligation to Fe^{III} (*30*, *31*), HRPC undergoes a transition from a five-coordinate high-spin to six-coordinate low-spin heme with a pK_a of 10.9 (*29*). Formation of low-spin heme in alkaline HRPC is promoted by H-bond donation by the Fe-bound OH^- ligand to the distal His42 (*30*) and stabilization of the OH^- ligand by Arg38 (*10*). The alkaline transition of (2.5 μM) HRPC is depressed by 25 mM BHA (Figure 4C), and also by BZA and NMBZA to the extent predicted by eq 3. This supports the role of Arg38 as an H-bond donor to the side chains of these substrates. Schonbaum (*2*) reported that hydroxamate anions do not bind to HRPC, which is reflected in the increased $K_{d(app)}$ values for BHA (61-fold) and 2-NHA (9-fold) between pH 8.0 and 10.0 (Table 2). SHA presents an interesting case since it has two groups that ionize between pH 4.0 and 12.0 (Figure 6). Table 2 reveals a 28-fold increase in the SHA $K_{d(app)}$ in the pH range (6.0−9.0) that brackets its pK_a at 7.4. The SHA^- monoanion can exit in three tautomeric forms with the negative charge located on the hydroxamate CO (**B**), N (**C**), or O (**D**) (Figure 6), and similar tautomers can be drawn for BHA^- and 2-NHA^- without the ring OH group. None of these tautomers is capable of simultaneously H-bonding to His42, Arg38, and Pro139 as observed in the HRPC−BHA complex, which would explain the reduced affinity of HRPC for the hydroxamate anions. The K_d values corrected for substrate ionization show little variation over the pH range of 4.0−12.0 (Table 3), which suggests that the enthalpy−entropy compensation seen at pH 7.0 and 4.0 (Table 1) operates over a wide pH range.

Nonpolar Interactions in the Binding of Aromatic Hydroxamic Acid Analogues to HRPC. Acetohydroxamic acid [K_d = 62 mM (*2*)] binds to HRPC >10^4-fold less tightly than BHA even though both compounds are capable of the same polyfunctional H-bonding. Enthalpically favorable van der Waals interactions, entropically favorable desolvation of the phenyl ring, and liberation of water molecules from the aromatic-binding pocket will all contribute to the binding energy of BHA being larger than that of acetohydroxamic acid. The effects of an increased level of nonpolar interactions can also be seen in the more favorable entropies of binding of 2-NHA and NMBZA, relative to those of BHA and BZA, respectively (Table 1). However, the unfavorable $\Delta\Delta H°$ for NMBZA versus BZA is attributed to steric effects of the bulky methyl group that destabilize the H-bond(s) in the distal cavity of the HRPC−NMBZA complex (Figure 1), and hence serve to increase the binding entropy.

Comparison of the crystal structures of HRPC and the HRPC−BHA complex shows that Phe68, which is located at the opening of the distal cavity, can adopt different conformations. It can flip away from the entrance toward the distal pocket (open conformation), or it can flip down and partially block the entrance (closed conformation) (*11*, *43*). Henriksen et al. (*11*) suggested that 2-NHA binding would be accommodated with Phe68 in the open conformation only, which would partly offset the entropic gain expected from desolvation alone. Therefore, the smaller $\Delta\Delta S°$ between 2-NHA and BHA (3.4 eu) compared to that between NMBZA and BZA (9.3 eu), which only differ by a CH_3 group, is assigned in part to a more rigid aromatic-binding pocket in the HRPC−2-NHA complex.

Effect of Ring Substituents on Hydrazide Binding to Ferric HRPC. The ortho-substituted hydrazides are the weakest to bind to HRPC (Table 4 and Figure 7). As proposed previously for SHA, H-bonding of the ring C2 group to Arg38 would account for the highly unfavorable $\Delta S°$ values (Table 4) for 2-OH-BZH (−37.9 eu) and 2-NH_2-BZH (−28.1 eu) versus BZH binding (−21.4 eu). Steric constraint between the ring C2 substituent and the hydrazide side chain in 2-CH_3-BZH and 2-Cl-BZH probably causes these substrates to be nonplanar. This would likely weaken the H-bonds formed with HRPC and contribute to their enthalpically less favorable binding versus BZH (Figure 7). The role of steric or electronic repulsion in decreasing the binding affinity of ortho-substituted substrates is supported by the high K_d (85 mM, Table 4) of 2-NO_2-BZH with its bulky NO_2 group.

With the exception of 3-NO_2-BZH, the meta-substituted hydrazides possess K_d values that differ from that of BZH by a factor of only ∼2 or less (Table 4). For both 3-OH-BZH and 3-NH_2-BZH, more negative enthalpies are largely compensated by more negative entropies (Figure 7). Such compensation may arise from H-bonding of these polar meta substituents with the carbonyl of Pro139 (Figure 1). Alternatively, they may donate H-bonds to Phe68 (Figure 1), which is close to the meta position of the BHA ring in its HRPC complex (*11*). Aromatic rings have been shown to be H-bond acceptors, forming H-bonds about half as strong as neutral H-bonds (*44*). The binding of 3-CH_3-BZH and 3-Cl-BZH to HRPC shows a reduction in enthalpy versus BZH similar to that of the corresponding ortho-substituted hydrazides but increased entropy (Figure 7), reflecting differences in the ability of the aromatic binding site to accommodate certain substituents, particularly unpaired (non-H-bonded) polar groups.

Examination of the HRPC−BHA structure shows that the phenyl rings of Phe68 and Phe179 are 3.70 and 3.93 Å, respectively, from C4 of the BHA ring (Figure 1). The binding parameters for 4-CH_3-BZH and 4-NH_2-BZH differ only slightly from those of BZH (Figure 7). In contrast, the binding of 4-OH-BZH and 4-Cl-BZH is accompanied by much larger (but compensatory) enthalpy and entropy changes relative to BZH. This can be attributed to increased flexibility in the complexes due to the unpaired (non-H-bonded) OH and Cl groups.

Binding of INH, NICH, and 2-NZH to Ferric HRPC. The thermodynamic parameters for INH and NICH are similar to those for 3-Cl-, 4-Cl-, and 4-OH-substituted BZH (Table 4), and their magnitudes relative to BZH can also be explained by desolvation effects. The pyridine N of free INH and NICH will be strongly H-bonded to water, and if we assume that the N atoms remain non-H-bonded in the complexes, the observed large enthalpic losses and entropic gains relative to BZH binding (Figure 7) are to be expected.

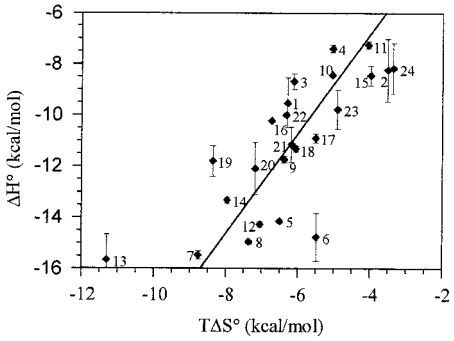

FIGURE 8: Plot of ITC $T\Delta S°$ vs $\Delta H°$ values for binding of the aromatic hydroxamic acid analogues to HRPC. Data for **1**−**7** and **8**−**24** from Tables 1 and 4, respectively (**1**, BZA; **2**, NMBZA; **3**, 2′-HA; **4**, N-BH; **5**, BHA; **6**, 2-NHA; **7**, SHA; **8**, BHA; **9**, BZH; **10**, INH; **11**, NICH; **12**, 2-NZH; **13**, 2-OH-BZH; **14**, 3-OH-BZH; **15**, 4-OH-BZH; **16**, 2-CH_3-BZH; **17**, 3-CH_3-BZH; **18**, 4-CH_3-BZH; **19**, 2-NH_2-BZH; **20**, 3-NH_2-BZH; **21**, 4-NH_2-BZH; **22**, 2-Cl-BZH; **23**, 3-Cl-BZH; and **24**, 4-Cl-BZH).

Tighter binding of the 2-NZH naphthyl ring in the aromatic-binding pocket of HRPC would provide a possible explanation for the relative magnitudes of the $\Delta H°$ and $\Delta S°$ values of 2-NHA and 2-NZH (Tables 1 and 4). Weaker binding of the hydrazide compared to that of the hydroxamate side chain in the distal cavity would allow optimization of the aromatic interactions in the HRPC−2-NZH complex. This would be enthalpically favorable but entropically unfavorable due to a further decrease in the flexibility of Phe68 and Phe179 in the aromatic pocket.

CONCLUSIONS

The linear relationship ($r^2 = 0.6$) in Figure 8 underscores the enthalpy−entropy compensation for the binding of aromatic hydroxamic acid analogues to HRPC. Such compensation is commonly observed for protein−small molecule interactions in aqueous solutions since the release of structured water molecules (desolvation) from the interacting surfaces results in an entropy gain that is offset by a loss in enthalpy due to enthalpically weaker H-bonds in bulk water (*45*). The net result is that $\Delta H°$ and $\Delta S°$ change proportionally, while $\Delta G°$ is less affected.

BHA, SHA, and 2-NHA binding to HRPC at neutral pH is clearly enthalpically driven, with the charged H-bond to Arg38 providing the largest contribution (up to ∼7 kcal/mol). The overall low substrate affinity of HRPC around neutral pH is due to unfavorable entropy terms (from −11.3 to −37.9 eu, Tables 1 and 4). This can be attributed to limited desolvation [∼7 eu is the maximum entropy gain from the release of a water molecule into the bulk solvent (*46*)] and decreased flexibility of the active site residues on substrate binding. Loss of flexibility in the distal Arg38, in particular, is highly entropically unfavorable as reflected in the binding entropies for BHA versus N-BH, and even more dramatically in those for SHA and 2-OH-BZH. Thus, the distal Arg38 can be viewed as an "entropic gate keeper" providing "entropic" protection to HRPC against the highly reactive

forms of its oxidized donor substrates generated during the normal peroxidase cycle.

The dramatic entropic gains observed at pH 4.0 (Table 1) likely reflect greater solvent access to the active site of HRPC. Also, the complexes are probably significantly less rigid at low pH as reflected in the much less favorable binding enthalpies. Substrates likely have greater access to the heme cavity of HRPC and other heme peroxidases at lower pHs, which, for example, may contribute to the rapid inactivation of lignin peroxidase at its pH optimum of 2−3 (*47*).

From the thermodynamic data presented here, the main obstacle to overcome in designing tight-binding peroxidase inhibitors is the large entropic barrier around neutral pH. Addition of a coordinating group with a high affinity for ferric heme iron, such as an isocyanide, may help overcome this entropic barrier. Alternatively, the design of a mechanism-based inhibitor may be a more productive approach.

REFERENCES

1. Veitch, N. C. (1995) *Biochem. Soc. Trans. 23*, 232−240.
2. Schonbaum, G. R. (1973) *J. Biol. Chem. 248*, 502−511.
3. La Mar, G. N., Hernandez, G., and de Ropp, J. S. (1992) *Biochemistry 31*, 9158−9168.
4. Sakurada, J., Takahashi, S., and Hosoya, T. (1986) *J. Biol. Chem. 261*, 9657−9662.
5. Veitch, N. C., and Williams, R. J. (1990) *Eur. J. Biochem. 189*, 351−362.
6. Veitch, N. C. (1993) in *Plant Peroxidases: Biochemistry and Physiology* (Welinder, K. G., Rasmussen, S. K., Penel, G., and Greppin, H., Eds.) pp 57−64, University of Geneva, Geneva, Switzerland.
7. Saxena, A., Modi, S., Behere, D. V., and Mitra, S. (1990) *Biochim. Biophys. Acta 1041*, 83−93.
8. Thanabal, V., La Mar, G. N., and de Ropp, J. S. (1988) *Biochemistry 27*, 5400−5407.
9. Smith, A. T., Sanders, S. A., Sampson, C., Bray, R. C., Burke, J. F., and Thorneley, R. N. F. (1993) in *Plant Peroxidases: Biochemistry and Physiology* (Welinder, K. G., Rasmussen, S. K., Penel, C. T., and Greppin, H., Eds.) pp 159−168, University of Geneva, Geneva, Switzerland.
10. Howes, B. D., Rodriguez-Lopez, J. N., Smith, A. T., and Smulevich, G. (1997) *Biochemistry 36*, 1532−1543.
11. Henriksen, A., Schuller, D. J., Meno, K., Welinder, K. G., Smith, A. T., and Gajhede, M. (1998) *Biochemistry 37*, 8054−8060.
12. Itakura, H., Oda, Y., and Fukuyama, K. (1997) *FEBS Lett. 412*, 107−110.
13. Welinder, K. G., and Gajhede, M. (1993) in *Plant Peroxidases: Biochemistry and Physiology* (Greppin, H., Rasmussen, S. K., Welinder, K. G., and Penel, C., Eds.) pp 35−42, University of Copenhagen, Copenhagen, Denmark, and University of Geneva, Geneva, Switzerland.
14. Tsukamoto, K., Itakura, H., Sato, K., Fukuyama, K., Miura, S., Takahashi, S., Ikezawa, H., and Hosoya, T. (1999) *Biochemistry 38*, 12558−12568.
15. Davey, C. A., and Fenna, R. E. (1996) *Biochemistry 35*, 10967−10973.
16. Davis, A. M., and Teague, S. J. (1999) *Angew. Chem., Int. Ed. 38*, 736−749.
17. Reddy, S. G., Scapin, G., and Blanchard, J. S. (1996) *Biochemistry 35*, 13294−13302.
18. Morgan, B. P., Scholtz, J. M., Ballinger, M. D., Zipkin, I. D., and Bartlett, P. A. (1991) *J. Am. Chem. Soc. 113*, 297−307.
19. Nakatani, H., and Takahashi, K. (1986) *Biochemistry 25*, 3515−3518.
20. Paul, K. G., and Ohlsson, P. I. (1978) *Acta Chem. Scand., Ser. B 32*, 395−404.
21. Hosoya, T., Sakurada, J., Kurokawa, C., Toyoda, R., and Nakamura, S. (1989) *Biochemistry 28*, 2639−2644.
22. Wiseman, T., Williston, S., Brandts, J. F., and Lin, L. N. (1989) *Anal. Biochem. 179*, 131−137.
23. Ortiz de Montellano, P. R. (1992) *Annu. Rev. Pharmacol. Toxicol. 32*, 89−107.
24. Kyte, J. (1995) *Mechanism in Protein Chemistry*, Garland Publishing, Inc., New York.
25. Jelesarov, I., and Bosshard, H. R. (1994) *Biochemistry 33*, 13321−13328.
26. Christensen, J. J., Hansen, L. D., and Izatt, R. M. (1976) *Handbook of proton ionization heats and related thermodynamic quantities*, Wiley, New York.
27. Holzbaur, I. E., English, A. M., and Ismail, A. A. (1996) *J. Am. Chem. Soc. 118*, 3354−3359.
28. Tsaprailis, G., Chan, D. W., and English, A. M. (1998) *Biochemistry 37*, 2004−2016.
29. Harbury, H. A. (1956) *J. Biol. Chem. 225*, 1009−1019.
30. Sitter, A. J., Shifflett, J. R., and Terner, J. (1988) *J. Biol. Chem. 263*, 13032−13038.
31. Feis, A., Marzocchi, M. P., Paoli, M., and Smulevich, G. (1994) *Biochemistry 33*, 4577−4583.
32. Fasman, G. D. (1975) *CRC Handbook of Biochemistry and Molecular Biology*, CRC Press, Cleveland, OH.
33. Fersht, A. R., Shi, J. P., Knill-Jones, J., Lowe, D. M., Wilkinson, A. J., Blow, D. M., Brick, P., Carter, P., Waye, M. M., and Winter, G. (1985) *Nature 314*, 235−238.
34. Kato, Y., Conn, M. M., and Rebek, J., Jr. (1995) *Proc. Natl. Acad. Sci. U.S.A. 92*, 1208−1212.
35. Habermann, S. M., and Murphy, K. P. (1996) *Protein Sci. 5*, 1229−1239.
36. Frisch, C., Schreiber, G., Johnson, C. M., and Fersht, A. R. (1997) *J. Mol. Biol. 267*, 696−706.
37. Edwards, S. L., and Poulos, T. L. (1990) *J. Biol. Chem. 265*, 2588−2595.
38. Larsen, I. K. (1978) *Acta Crystallogr. B34*, 962−964.
39. Rodriguez-Lopez, J. N., George, S. J., and Thorneley, R. N. F. (1998) *J. Bioinorg. Chem. 3*, 44−52.
40. Shiao, D. D., and Sturtevant, J. M. (1976) *Biopolymers 15*, 1201−1211.
41. Smulevich, G., Paoli, M., De Sanctis, G., Mantini, A. R., Ascoli, F., and Coletta, M. (1997) *Biochemistry 36*, 640−649.
42. Priori, A. M., Indiani, C., De Sanctis, G., Marini, S., Santucci, R., Smulevich, G., and Coletta, M. (2000) *J. Inorg. Biochem. 79*, 25−30.
43. Gajhede, M., Schuller, D. J., Henriksen, A., Smith, A. T., and Poulos, T. L. (1997) *Nat. Struct. Biol. 4*, 1032−1038.
44. Levitt, M., and Perutz, M. F. (1988) *J. Mol. Biol. 201*, 751−754.
45. Lumry, R., and Rajender, S. (1970) *Biopolymers 9*, 1125−1127.
46. Dunitz, J. D. (1995) *Chem. Biol. 2*, 709−712.
47. Tuisel, H., Sinclair, R., Bumpus, J. A., Ashbaugh, W., Brock, B. J., and Aust, S. D. (1990) *Arch. Biochem. Biophys. 279*, 158−166.
48. Fukada, H., and Takahashi, K. (1998) *Proteins 33*, 159−166.

BI010445F